Cement & Concrete Composites 34 (2012) 529–537

Contents lists available at SciVerse ScienceDirect

Cement & Concrete Composites

journal homepage: www.elsevier.com/locate/cemconcomp

Reliable onset time determination and source location of acoustic emissions in concrete structures

A. Carpinteri, J. Xu *, G. Lacidogna, A. Manuello

Politecnico di Torino, Department of Structural Engineering and Geotechnics, Corso Duca degli Abruzzi 24, 10129 Torino, Italy

ARTICLE INFO

Article history:
Received 4 September 2010
Received in revised form 23 November 2011
Accepted 24 November 2011
Available online 30 November 2011

Keywords:
Acoustic emission
Onset time determination
Akaike Information Criterion
Certainty degree
Apparent velocity
Crack location

ABSTRACT

Acoustic emission (AE) technique, as an effective method to monitor the crack characterization in concrete materials is investigated in this paper. An improved approach, based on the Akaike Information Criterion (AIC), is proposed to provide more reliable onset time determination of AE signals. The introduced parameters, quantification of the certainty degree and the apparent velocity in the improved method can help to eliminate the false or doubtful picked onset results automatically. The improved AIC method is successfully applied to the AE detection during a three-point bending test of a fiber reinforced concrete beam to analyze the crack pattern. It is shown that the proposed method is a reliable tool for automatic onset time determination and useful for the crack source location in concrete structures.

1. Introduction

Various concrete and reinforced concrete materials are being increasingly employed in structural applications. Concrete structures could deteriorate due to fatigue, chemical reactions, unpredictable disasters, poor workmanship, etc., although the concrete structures have long been referred to as maintenance-free [1–3]. Therefore, monitoring techniques are progressively assuming greater importance in the field of structural engineering. Acoustic emission (AE) techniques are usually adopted among the non-destructive methods, since they allow passive observation of crack growth or internal defects [4]. The source of AE activity generated by the crack propagation in the concrete is closely connected to the model of fracture [5,6]. If the dominant mode is determined, it is possible to reinforce the structure using proper design or materials with resistance against the specific cracking mode. In this regard, acoustic emission (AE) techniques have been extensively studied in numerous applications for damage characterization of concrete materials and structures [7–11].

In the application of AE techniques, sensors are placed on the structural surface to record the transient waves (hits) generated by the crack incidents inside materials. Subsequently, the characterization and quantification of the damage level are performed via the use of appropriate AE descriptors. Further study of the transient waveforms provides in-depth insight of the fracture process [4,12]. Onset time determination of a transient signal is important in this technique, since it directly results in the accuracy of crack event location and source mechanism analysis [13]. The true onset time of a crack AE event could be described as the moment when the first energy of a particular signal phase reaches the sensor positions [4,14]. In the signal analysis, the onset time is usually picked as the point where the first difference between the signal and the noise takes place [14]. It is necessary to have reliable automatic picking tools, because human analysts cannot manage the vast amount of data recorded in the whole monitoring process.

Therefore, various algorithms have been proposed for automatic detection of onset times. Most of the methods are from the seismology after some modifications, since seismology and AE measurement are related fields [15]. The simplest form for onset picking is to use an amplitude threshold-picker [16]. In this method, some special value is set for amplitude of signal as the threshold, and the onset time is determined as the time when the value of the corresponding amplitude exceeds the threshold value. However, the result from this method is very rough and sometimes is not available for a pure threshold approach, such as small amplitude signals and/or signals with a high noise level. Another approach using a dynamic threshold is the so-called STA/LTA (STA – Short Term Average, LTA – Long Term Average) picker by [17]. Here, STA measures the instant amplitude of the signal and LTA contains information about the current average acoustic noise amplitude. With the same idea, different forms of STA/LTA are defined. Due to the fact that signal and noise of acoustic emissions in concrete are often to be found in the same frequency range (20–500 kHz), the STA/LTA picker

* Corresponding author. Tel.: +39 3208371837; fax: +39 0115644899.
E-mail address: jie.xu@polito.it (J. Xu).

0958-9465/$ - see front matter © 2011 Elsevier Ltd. All rights reserved.
doi:10.1016/j.cemconcomp.2011.11.013

would not produce accurate enough results [14]. Modeling the signal as an autoregressive (AR) process is another approach for onset time determination. It is based on the so-called Akaike Information Criterion (AIC) picker [18]. In this case, the intervals of the AE signal before and after the onset time are assumed to be two different stationary datasets. For a fixed order AR process, the point, at which the AIC is minimized, determines the separation of the two time series and therefore the probable onset time can be found [19,20]. Some other methods based on different mechanisms, such as artificial neutral network [21], fractal dimension [22], spectrograms [23] and Hinkley criterion [14], are also proposed. Among the aforementioned methods, the AIC algorithm is proven to be a more accurate and suitable one in concrete structures [14,20].

Although these methods can automatically determine the onset time of AE signal, they cannot check the validity of the detected times. The accuracy of these methods can be only calibrated before the monitoring and this is not enough. Because the number of recorded AE signals can be up to several thousand during the test and false recognition of arrival times is unavoidable in the automatic analysis [14]. Thus, it is important not only to pick onset times with better accuracy but also to eliminate the false or doubtful picks automatically by checking the validity of the detected result.

In this paper, an improved procedure (or improved AIC-picker) based on the AIC-picker is proposed for the automatic processing system of AE technique to eliminate false or doubtful picks. The improved AIC-picker is based on the degree of accuracy of AE signals, which can be estimated by the second derivative of the AIC function, as shown for seismic signals by Maeda [24], and by another parameter related to the propagation velocity of the AE in the monitored structure. The AE signals generated during ad hoc tests, were detected by the improved AIC-picker and compared to manual picking determination in order to evaluate the validity of the algorithm. Finally, the improved AIC-picker has been successfully applied to AE analysis in a three-point bending test of a fiber reinforced concrete beam.

2. Basic principle of the AIC-picker

Picking the onset times is equivalent to dividing a section which contains a phase onset into two parts in time series. For the dividing criterion, the *Akaike Information Criterion* (AIC) was introduced by [19]. AIC, which was derived by [18], is defined as following equation:

$$\mathrm{AIC} = -2\ln(L) + 2k, \tag{1}$$

where k is the number of parameters in the statistical model, and L is the maximized value of the likelihood function for the estimated model. Generally, a model with minimum AIC value is thought to be the most suitable one among the competing models [19]. The method to establish the model is mainly based on that of Kitagawa and Akaike [25], in which a time series is divided into locally stationary segments and each is modeled as an AR process. The technique assumes that we have a time series $x_n = \{x_1, \ldots, x_n\}$, which includes the onset of an acoustic signal and a first estimate of the onset time. The intervals before and after the onset time are assumed to be two different stationary time series.

As illustrated in Fig. 1, the section with n points is divided into two parts, and MODEL 1 and MODEL 2 are fitted to the former part (from 1st point to kth point) and the latter part (from $(k+1)$th point to nth point) with the maximum likelihood estimation, respectively.

Then, the AIC value (denoted by $AIC(k)$) is calculated for this case. The point which gives minimum value to $AIC(k)$ is searched for, and the corresponding time to this point is regarded as the onset time. If the AIC value is calculated for MODEL 0 fitted to a whole

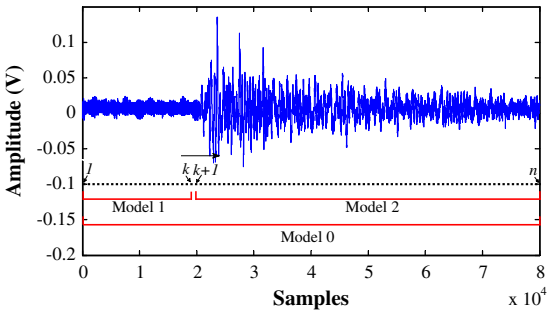

Fig. 1. Illustration of the method to divide a time series of an AE signal.

section, we can judge whether the section should be divided or not by the comparison between the minimum value of $AIC(k)$ and the AIC value for MODEL 0. The global minimum of the AIC function defines the onset point of the signal (Fig. 2).

In each interval $i = 1, 2$, the one preceding and the one including the phase onset, we define a model window in which we fit the data to an AR model of order M with coefficients $a_m^i (m = 1, \ldots, M)$:

$$x_t = \sum_{m=1}^{M} a_m^i x_{t-m} + e_t^i \tag{2}$$

with $t = 1, \ldots, k$ for interval 1 and $t = k+1, \ldots, n$ for interval 2. The model divides the time series within a model window into a deterministic and a non-deterministic part. The non-deterministic time series e_n^i or noise, is supposed to be Gaussian, with mean $E\{e_n^i\} = 0$, variance $E\{(e_n^i)^2\} = \sigma_i^2$ and uncorrelated with the deterministic part of the time series: $E\{e_n^i x_{t-m}^i\} = 0$.

The maximum likelihood estimation (MLE) is used to extract the non-deterministic part of the time series in intervals $[1, k]$ and $[k+1, n]$ using Eq. (2), where k is the division point. As we assume the non-deterministic parts to be Gaussian, we can express the approximate likelihood function L for the two non-deterministic time series in intervals $[1, k]$ and $[k+1, n]$ as:

$$L(x; k, M, \Theta_i) = \prod_{i=1}^{2} \left(\frac{1}{\sigma_i^2 2\pi}\right)^{n_i/2} \times \exp\left(-\frac{1}{2\sigma_i^2} \sum_{j=p_i}^{n_i} \left(x_j - \sum_{m=1}^{M} a_m^i x_{j-m}\right)^2\right) \tag{3}$$

where $\Theta_i = \Theta(a_1^i, \ldots, a_M^i, \sigma_i^2)$ represents the model parameters (σ_i^2 is dependent on k), and $p_1 = 1$, $p_2 = k+1$, $n_1 = k$, $n_2 = n - k$. Taking

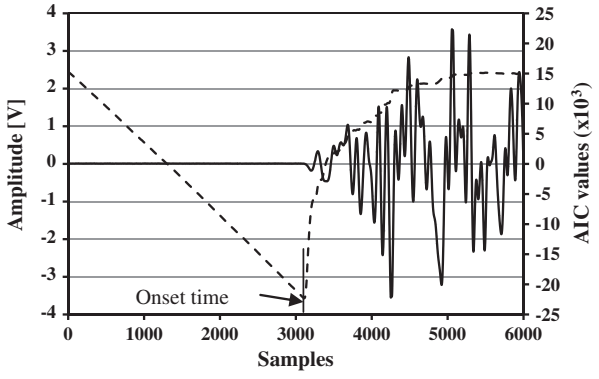

Fig. 2. The AIC value is used for onset determination only for the selected part of the signal containing the onset denoted by the solid line. The minimum value of the AIC function represented by the dashed line denotes the onsets time of the signal.

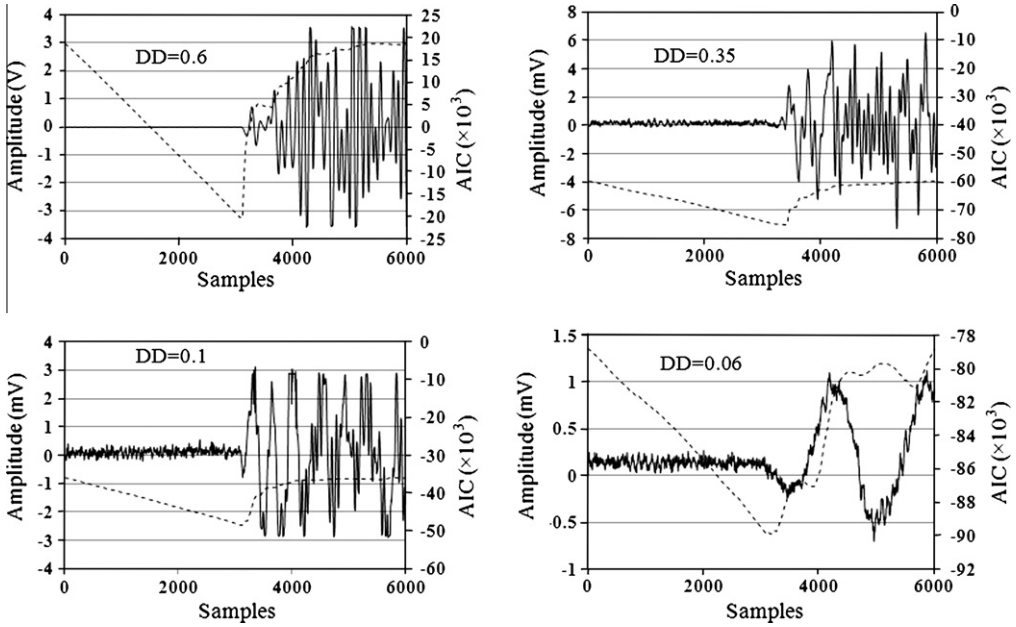

Fig. 3. Examples of picking *P*-times by *AIC*(*k*) and the corresponding *DD* values. The solid line is the signal and the dashed line is the AIC value.

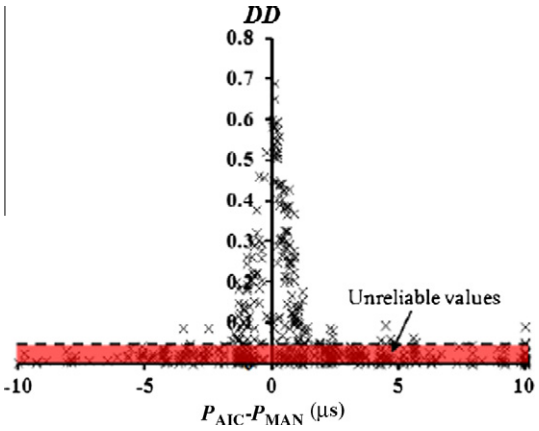

Fig. 4. *DD* value versus *P*-time picked automatically by *AIC*(*k*) minus *P*-time picked manually. Points at 10 μs represent the cases where the absolute value of the difference is greater than 10 μs.

the logarithm of Eq. (3) and searching for the maximum likelihood estimation of the model parameters we get:

$$\frac{\partial \ln L(x;k,M,\Theta_i)}{\partial \Theta_i} = 0 \tag{4}$$

which has the solution:

$$\sigma^2_{i,\max} = \frac{1}{n_i}\sum_{j=p_i}^{n_i}\left(x_j - \sum_{m=1}^{M} a^i_m x_{j-m}\right)^2 \tag{5}$$

The maximum of the logarithmic likelihood function for the two models as function of k becomes:

$$\begin{aligned}\log L(x;k,M,\Theta_1,\Theta_2) &= -\tfrac{n_1}{2}\log\left(\sigma^2_{1,\max}\right) - \tfrac{n_2}{2}\log\left(\sigma^2_{2,\max}\right) - \tfrac{n}{2}(1+\ln 2\pi)\\ &= -\tfrac{k}{2}\log\left(\sigma^2_{1,\max}\right) - \tfrac{(n-k)}{2}\log\left(\sigma^2_{2,\max}\right) + C\end{aligned} \tag{6}$$

where C is a constant. When n is large enough, the influence of the constant C can be neglected. Considering the AIC in Eq. (1), the AIC of the two-interval model is given as function of merging point k:

$$AIC(k) = k\log\left(\sigma^2_{1,\max}\right) + (n-k)\log\left(\sigma^2_{2,\max}\right) + 2C \tag{7}$$

Originally, this function was designed to determine the order of the AR process in Eq. (2). The first term indicates the badness of the model fit and the second the unreliability [18]. In our application, we have fixed the order to M, therefore this function is a measure for the model fit. Point k where the joint likelihood Eq. (6) is maximized, or *AIC*(*k*) in Eq. (7) is minimized, determines the optimal separation of the two stationary time series. This division point leads to the best fit for both models in the least squares sense, and is interpreted as the phase onset.

Theoretically, onset times of the *P*-waves (longitudinal waves) and *S*-waves (shear waves) can be used for crack characterization. However, only first wave onset times (*P*-wave times) are usually measurable, since multiple side reflections, structural noise and sensor response will interfere the later phases. Therefore, a proper time window that contains the onset time should be chosen if only the onset of *P*-wave is to be determined. In practice, this method is denoted as AIC-picker and the *AIC*(*k*) value is defined as:

$$\begin{aligned}AIC(k_w) = {} & k_w \log(\mathrm{var}(R_w(1,k_w))) + (n_w - k_w)\log(\mathrm{var}(R_w(1\\ & + k_w, n_w))),\end{aligned} \tag{8}$$

where the subscript w denotes that not the whole time series is taken, but only the chosen window containing the onset time. n_w, is the last sample of the current time series, k_w ranges from 1 to n_w. The term var($R_w(1, k_w)$) is the variance function calculated from 1 to k_w, while var($R_w(1 + k_w, n_w)$) means that all samples ranging from $1 + k_w$ to n_w are considered. The global minimum of the AIC function defines the first *P*-wave onset time of the AE signal, shown in Fig. 2.

3. Picking the onset times of *P*-waves (*P*-times)

3.1. Setting time windows

As mentioned before, AIC-picker gives higher quality if the AIC is only applied to a pre-selected window of the time series containing the onset time [20]. To do this, in the automatic algorithm fine tuned by the authors, the *P*-time is firstly pre-determined by a simple method using a threshold amplitude level:

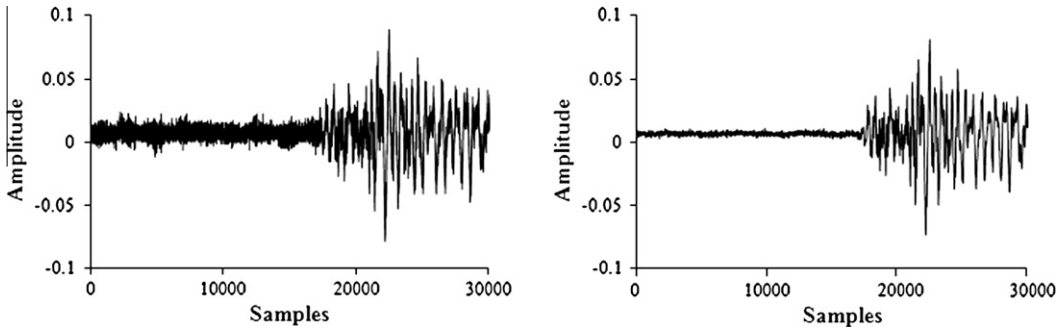

Fig. 5. Raw acoustic emission signal (left) and low-pass filtered acoustic emission single (right).

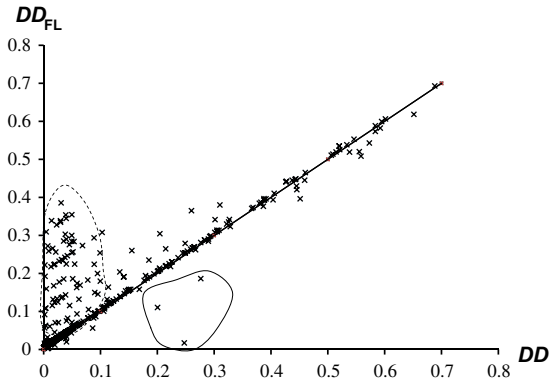

Fig. 6. A relation of *DD* value for filtered data versus that for non-filter wave data. Plots surrounded by a broken line represent the cases that filtering is highly successful in picking *P* times for the signals. Plots surrounded by a solid line represent the cases that filtering produces bad result.

$$\left(\sum_{t=k+1}^{10}|x_t|\right)\Big/10 \geqslant 4\left(\sum_{t=1}^{k}|x_t|\right)\Big/k \tag{9}$$

By means of this relation, the mean amplitude of a shifting set of 10 data is compared with the fourfold mean amplitude of the interval of the time series ranging from 1 to k. The first value of k, which satisfies Eq. (9), is selected as the pre-determined onset time (k_0). The first estimation is always localized after the actual onset time. Taking into account this point in the AIC application, two kinds of time windows with different time intervals are set sequentially. First, we apply the algorithm to the interval $[1,k_0]$ (window 1), which is used for a rough determination of the onset time by the AIC and gives k_1 value. The second time window (2) is considered centered on the value k_1 with a length of $2\Delta k$. The value of Δk depends on the sample frequency. In our study, the sample frequency is 10 MHz, and Δk equal to 3000 samples gives us an ideal result. The onset time, corresponding to the value $k_{\min}$ coming from the AIC-picker to the time window (2), is considered as the actual onset time of the AE signal analyzed.

3.2. Quantification of the certainty degree

The certainty degree of the onset time improves the preciseness of AE damage location and can be estimated by the certainty parameter *DD* [24]. This parameter, represented by the second derivative of the AIC function at the onset time, is defined as follows:

$$DD = (AIC(k_{\min}-\delta k)+AIC(k_{\min}+\delta k)-2AIC(k_{\min}))/(\delta k)^2 \tag{10}$$

where $k_{\min}$ is the point which gives the minimum value to $AIC(k)$ and δk is defined as the number of points corresponding to a small time interval. As the wave data used in this study, δk is set at 150.

Sensor	1	2	3	4	5	6	7	DD≥0.5	Sum
1	-	0	0	1	0	0	1	Y	2
2	0	-	0	3	0	0	3	N	6
3	0	0	-	1	0	0	1	Y	2
4	3	3	3	-	3	3	0	N	*15*
5	0	0	0	1	-	0	1	Y	2
6	0	0	0	1	0	-	0	Y	1
7	3	3	3	0	3	0	-	N	12

Not reliable

Sensor	1	2	3	5	6	7	DD≥0.5	Sum
1	-	0	0	0	0	1	Y	1
2	0	-	0	0	0	3	N	3
3	0	0	-	0	0	1	Y	1
5	0	0	0	-	0	1	Y	1
6	0	0	0	0	-	0	Y	0
7	3	3	3	3	0	-	N	*12*

Not reliable

Sensor	1	2	3	5	6	DD≥0.5	Sum
1	-	0	0	0	0	Y	0
2	0	-	0	0	0	N	0
3	0	0	-	0	0	Y	0
5	0	0	0	-	0	Y	0
6	0	0	0	0	-	Y	0

Fig. 7. An example to check the validity of the picked onset times by *DD* value and apparent velocity V_{ij}.

Fig. 3 shows some typical AE signals together with the $AIC(k)$ function denoted by the dashed line. For each case, the *DD* value is computed. The greater the *DD* value, the more precise the onset determination. For the AE signal reported in Fig. 3a, the signal-to-noise ratio is relatively high, the peak of the AIC function is particularly sharp and the *DD* parameter is assumed equal to 0.6. In the other cases (see Fig. 3b–d), where the noise is even more appreciable, the signal-to-noise ratio is much lower, the *DD* values are smaller.

In order to define the discriminating value, ad hoc tests were conducted in Section 4.1. In Fig. 4, the *DD* values and the difference between the onset times computed automatically and manually are reported, considering AE artificially generated on the surface of a concrete specimen. The difference between the onset times computed by the two different procedures are reported in microseconds (μs) into the graph. It shows that the *DD* values are lower than 0.05, and very large differences (>10 μs) exist. Accordingly, the accuracy of *P*-time can be examined by checking whether *DD* value is smaller than 0.05 or not.

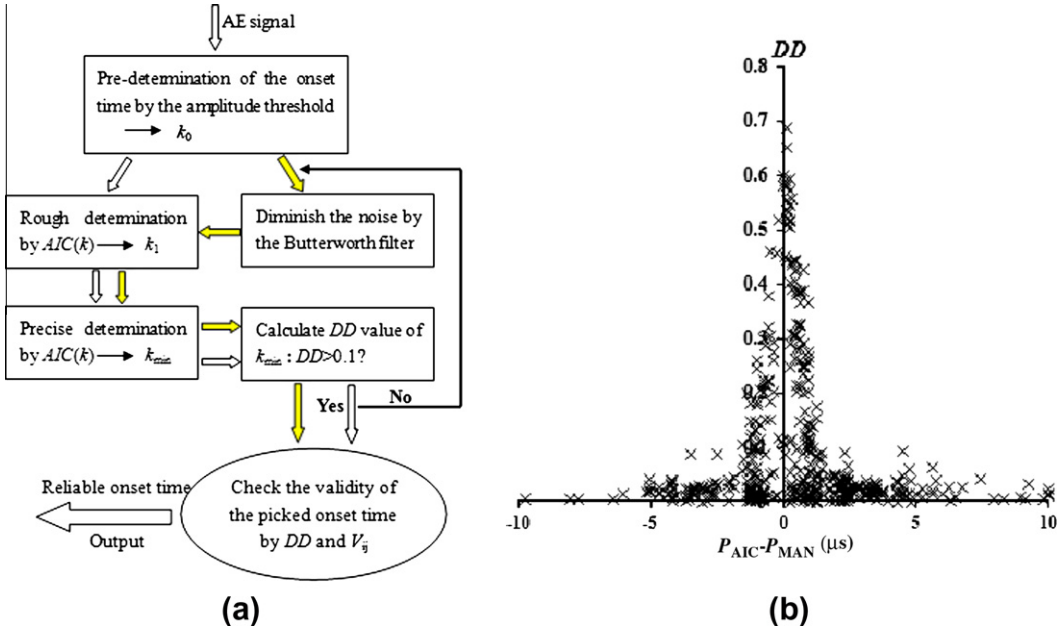

Fig. 8. (a) Flow-chart of the improved AIC-picker to determine *P*-times; (b) results of picking *P*-times following the procedure shown in (a). See Fig. 4 caption for explanation for the figure contents.

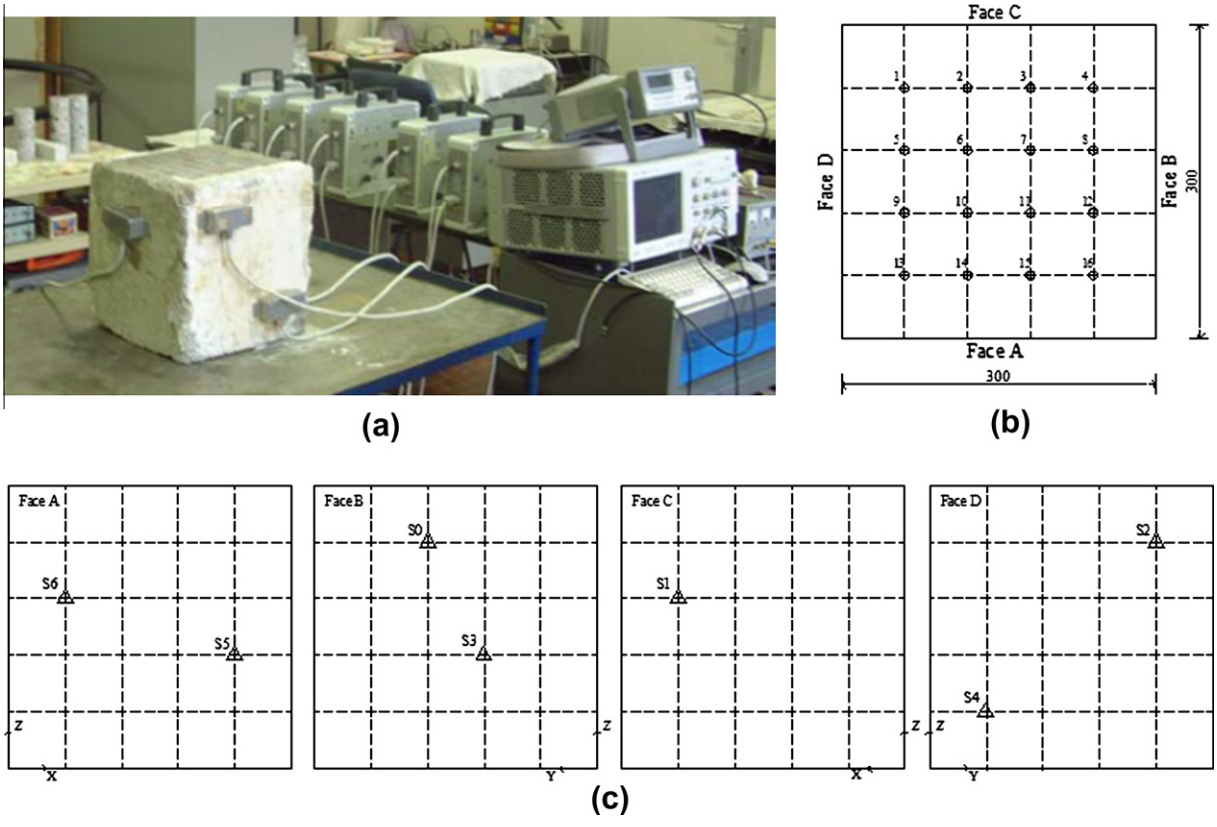

Fig. 9. Concrete cube with AE sensors applied on lateral faces. (a) The test 300 × 300 × 300 mm^3 concrete cube and the test equipments. (b) The 16 artificial source positions of the pencil–lead break. (c) Positions of the sensors on the four lateral faces.

3.3. Adoption of low cut filter

Acoustic emissions and seismograms have many similarities. However, there also exist differences, which do not allow the exact application of the same picking algorithms in both fields. Concerning seismic events, for instance, signal and noise are usually located in different frequency ranges. Therefore, we can eliminate the noise through a simple Fourier transform and corresponding

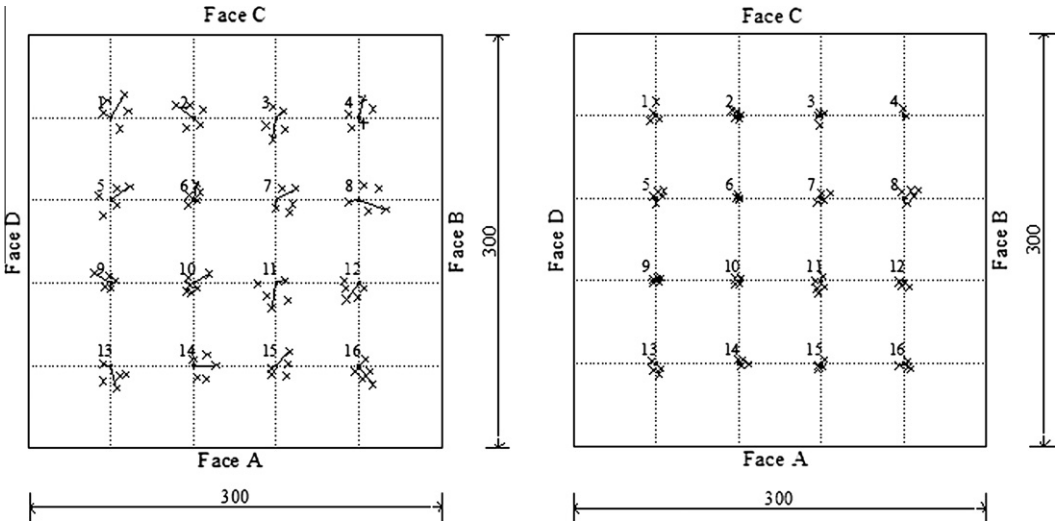

Fig. 10. Location results using *P*-wave onset times and the seven sensors. Left is the result of the AIC-picker. Right is the result of the improved AIC-picker by *DD* and V_{ij}. The cross points are the tested positions from the pickers and the dot point is the real source positions.

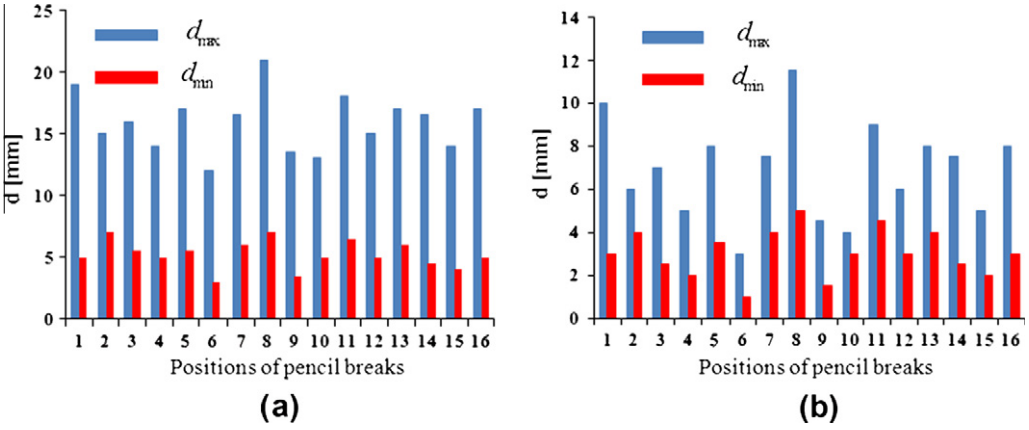

Fig. 11. Comparison between the maximum (d_{max}) and the minimum (d_{min}) errors at each position of pencil breaks using the onset times of *P*-waves: (a) using the AIC-picker; and (b) using the improved AIC-picker.

filter, which produces reliable results. Different from that, the application of AE in concrete, signal and noise, are often in the same frequency range (20–500 kHz).

If we try to eliminate the noise, the real single will be influenced unavoidably, and reduces the first motion and distorts the true onset time of *P*-wave [26]. Therefore, it is necessary to diminish the noise as much as possible instead of eliminating it. In the above consideration, Butterworth low-pass filter is used. Fig. 5 shows that Butterworth filter can diminish the noise effectively in advance.

The filtering effect for picking was investigated by using the *DD* value defined above. Fig. 6 shows a relation between *DD* values for filtered and non-filtered wave data.

In Fig. 6, it suggests that the filtering is effective in picking *P*-times as a whole. In particular, when *DD* values are smaller than 0.1, the filtering effect is very successful, such as the plots surrounded by a dashed line in Fig. 6. Nevertheless, we must not forget the case that the filter makes the results of picking very bad, such as the plots surrounded by a solid line in Fig. 6. Accordingly, it is decided that the filtered wave data should be used when the following condition is satisfied:

$$DD_{FL} > DD_{Non} \;\&\; DD_{Non} < 0.1 \qquad (11)$$

Table 1
Percentage of events with a deviation greater than 5 mm from the exact locations for each coordinates axis.

Coordinates axis	Manually (%)	Improved AIC-picker (%)	AIC-picker (%)
x	0.6	3	9
y	0.9	3	11
z	1.2	4	11

where DD_{FL} and DD_{Non} represent the *DD* values for filtered and non-filtered wave data, respectively. Usually, picks from the filtered data are adopted; otherwise picks from the non-filtered data are adopted when Eq. (11) is not satisfied.

3.4. Apparent velocity

In addition to the *DD* value, the other parameter, an apparent velocity V_{ij}, can be considered to exclude doubtful and incorrect data. The apparent velocity can be computed by taking into account the onset times, which are obtained by the AIC and the distance between a couple of sensors *i* and *j* recording the same AE event, i.e.:

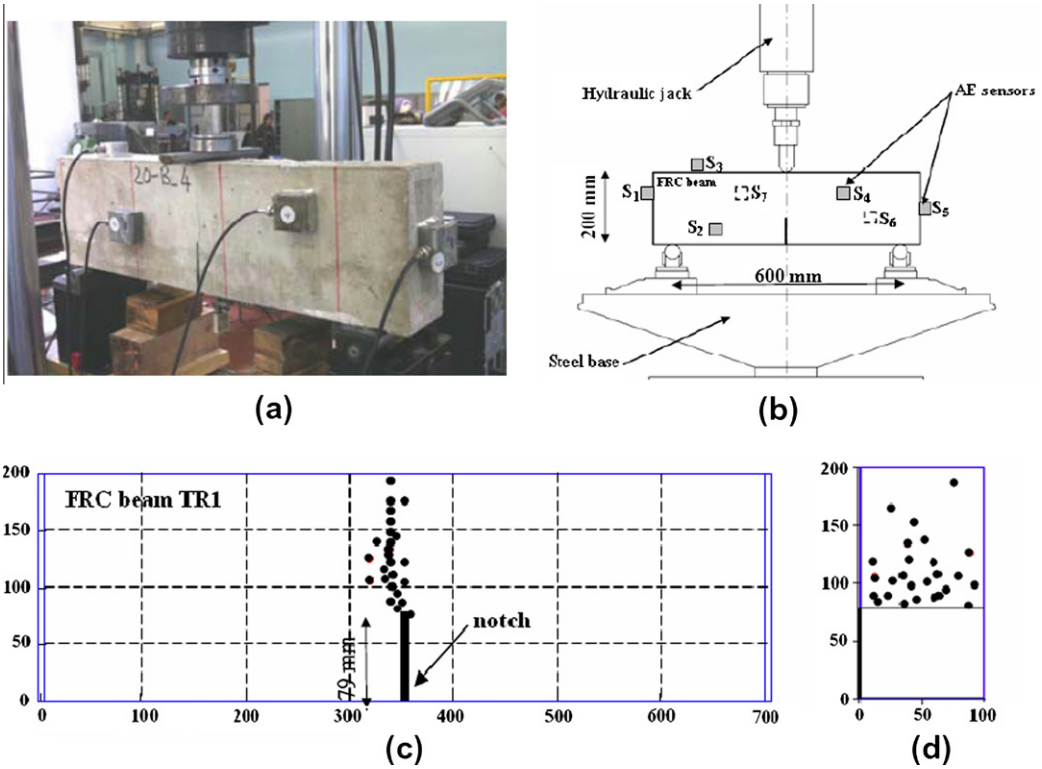

Fig. 12. (a) Three point bending test and AE sensor positions. (b) Scheme of the test. (c and d): AE source locations: During the tests, 26 AE sources were located by the improved AIC-picker.

$$V_{ij} = R_{ij}/|t_i - t_j| \tag{12}$$

where R_{ij} denotes the distance between the sensors i and j sensors, t_i and t_j are respectively the onset times computed for the AE signal recorded by the two sensors. If the apparent velocity is smaller than a certain value, depending on the material property of the monitored element, one of the two onset times is considered unreliable.

In the case of concrete structures, the comparison value for the apparent velocity is set to 4×10^3 m/s, and it coincides with the propagation velocity of elastic waves in plain concrete [13]. When V_{ij} is larger than 4.0 km/s, a score 0 is given to both ith and jth sensors; otherwise, a score 1 is given to them. At the same time, if DD value for a sensor out of them is less than 0.05, 2 is added to the score of the sensor. Elements in the table represent scores calculated for all pairs of sensors. Sum of scores for each sensor is calculated. P-time of the sensor with the largest score among the sensors is eliminated. Such an operation of omitting P-time is continued until all elements in table become zero.

Fig. 7 shows an example of about the apparent velocity. Three steps are shown in the case in which the sensor array is constituted by seven sensors that receive seven signals from the same AE event. In this case, the purpose of the improved procedure is to determine the accuracy of the onset time automatically by the AIC-picker. The reliability level of the signal can be evaluated by the two parameters (DD and V_{ij}) attributing an uncertainty score equal to unity if the computed apparent velocity is less than 4×10^3 m/s, and another score equal to 2 if the DD value is smaller than 0.05. The apparent velocity expressed by Eq. (12) is calculated for all the possible pairs of detecting transducers. The total value for a signal detected by the generic sensor is obtained by summing the uncertainty level 0 or 1 for the parameter V_{ij} and 0 or 2 for the parameter DD. In the first step, we find that sensor 4 reaches the higher uncertainty level with a value of 15. Obviously, considering two sensors, when a score of 3 is reached both the uncertainty conditions (DD and V_{ij}) are not satisfied. For this reason, in the first step sensor 4 is neglected. Then, this procedure is repeated considering the left sensors 1, 2, 3, 5, 6 and 7. In the second step, the higher uncertainty level is reached by sensor 7 with a score of 12, and this sensor will not be considered anymore. The process stops when signal detected by each sensor has a 0 score. In the analyzed case, this optimal condition is reached at the third step, where the onset time computed by sensors 1, 2, 3, 5 and 6 can be used for the location procedure.

3.5. Procedure of improved AIC-picker and picking results

Fig. 8a shows that the procedure to determine the onset times by the improved AIC-picker, obtained after the discussion from 3.1 to 3.4.

Fig. 8b shows that the results of picking of P-times follow the procedure as shown in Fig. 8a. It is obvious that the results in Fig. 8b are fairly good with the comparison of that in Fig. 4.

4. Application of the improved AIC-picker to experiment tests of the crack source location

Considering an AE event generated at point S at time t_0. Let us donate with t_i the time of arrival at a sensor S_i of the event, thus:

$$|S - S_i| = \left[(x - x_i)^2 + (y - y_i)^2 + (z - z_i)^2\right]^{1/2} \tag{13}$$

Assuming the material to be homogenous, the distance between S_i and source S, in Cartesian coordinates, is given by: $|S - S_i| = v_p(t_i - t_0)$. If the same event is observed from another sensor S_j at time t_j, it is possible to eliminate t_0 from the calculation [13]:

$$|S - S_i| - |S - S_j| = v_p(t_j - t_i) = v_p \Delta t_{ij} \quad (14)$$

If the onset times of the signals and the positions of the two sensors are known, Eq. (14) is with four unknowns, x, y, z and v. Hence, the location of S is a problem that can be solved in an exact manner, if there are enough equations as Eq. (14). Traditionally, a minimum number of five transducers have to be employed to univocally determine the three source coordinates and the P-wave propagation velocity [13]. The corresponding system of nonlinear equations is solved by an iterative algorithm. Applying a least squares approach, time residuals at the different transducers are calculated and random measurement errors can be recognized [13,14].

4.1. Pencil–lead break test

The onset time determination can be obtained by the improved AIC-picker shown in the previous section and can also be included into the automatic location procedure. Ad hoc tests were performed to reproduce AE using pencil–lead break in small and predictable regions of a concrete specimen [27]. A concrete cube with side length of 300 mm was cast at the Fracture Mechanics Laboratory of the Politecnico di Torino (Fig. 9a). Seven AE sensors were applied to the external surfaces of the concrete element (Fig. 9c). In particular, a grid corresponding to 16 points (artificial sources) was drawn on the upper face of the specimen (Fig. 9b).

The tip of a pencil was broken five times at each point, so there are total of 80 measurements for 16 points on the upper surface of the cube. From this experiment 560 AE events from the seven sensors were obtained for a comparative investigation. The onset times of the 560 events were picked manually as well as automatically using the AIC-picker and the improved AIC-picker shown in the previous section.

The results of the location are shown in Fig. 10. It can be noted that the events localized with the AIC-picker are not all located close to the real positions of the pencil breaks (Fig. 10a). The maximum and minimum errors observed in the 80 measurements for each of the break points are shown in Fig. 11. The events from the improved AIC-picker give more reliable results, although some of them are eliminated after the onset determination. Furthermore, in Table 1, the deviation of all the results obtained by the AIC-picker and the improved AIC-picker are reported. Considering the results summarized in Table 1, it is possible to conclude that AIC-picker presents a maximum deviation of 11% for y and z coordinates of the sources, whereas the improved AIC-picker gives more accurate results, of which the largest deviation is equal to 4%. The validity of the onset time determination using the improved AIC-picker is confirmed to be effective in increasing the accuracy of the location of AE sources in damaged concrete structures.

4.2. Three-point bending test on the fiber-reinforced concrete beam

The improved AIC-picker is also employed to determine the onset times of AE events generated during a three-point bending test of a steel fiber-reinforced concrete (FRC) beam (fiber content: 20 kg/m^3). The FRC beam is monitored by seven AE piezoelectric transducers, working in a frequency range between 20 kHz and 500 kHz, and they are applied on the external surface of the element as shown in Fig. 12a and b. The onset times of the AE signals detected during the test are successfully used in the location procedure to determine the crack positions in the FRC element. The monitored notched beam was loaded up to failure by controlling the crack mouth opening displacement (CMOD) with an opening velocity equal to 0.001 mm/s. The geometrical characteristic of the beam and the testing scheme are reported in Fig. 12b–d.

As for the AE monitoring, a total number of 26 AE points was localized by means of the triangulation based on the improved AIC-picker. A very good agreement is obtained between the localized points and the crack pattern configuration (see Fig. 12c and d).

5. Conclusion and outlook

With wide applications of concrete materials, the monitoring techniques have received considerable attention due to the increasing demand of the structural retrofit and strengthening. As one of the non-destructive monitoring techniques, acoustic emission technique is extensively employed for the concrete cracking analysis.

Reliable and exact onset time determination is important in the AE techniques, since it is the premise for the interpretation of the corresponding results in the damage evaluation of concrete structures. The huge amount of data gained during one test makes automatic onset detection a highly preferable status. The existing methods used for automatic picking of AE arrival time cannot check the validity of each detected AE signal. The improved AIC-picker proposed in this paper allows determining a degree of uncertainty, which is useful to eliminate false or doubtful onset times by the two parameters, i.e., the degree of certainty DD and apparent velocity V_{ij}.

The results of an ad hoc experiment have shown that the deviations of the results obtained by the improved method ranging from 3% to 4% from the correct results. This evidence allows considering the proposed method as the most accurate and suitable one among the onset determination methods of AE signals available. In addition, the AE source location algorithm, based on the improved AIC-picker, can be included in a computer procedure for AE data analysis. These methods can be very useful for a telematic working approach, using wireless transmission systems, where efficient algorithms for processing a large amount of data are in need.

Acknowledgments

We wish to thank Prof. Maeda from Kyoto University to provide us the papers which inspire our study. The authors also thank Dr. Chen and Dr. Niccolini for their help in the test and appreciate their suggestions. The financial support provided by the Regione Piemonte (Italy) RE-FRESCOS Project is gratefully acknowledged.

References

[1] Redmond DF, Christer AH, Rigden SR, Burley E, Tajelli A, Abu-Tair AOR. Modelling of the deterioration and maintenance of concrete structures. Eur J Oper Res 1997;99(3):619–31.
[2] Liu T, Weyers RW. Modeling the dynamic corrosion process in chloride contaminated concrete structures. Cement Concr Compos 1998;28(3):365–79.
[3] Spragg RP, Castro J, Li W, Pour-Ghaza M, Huang P-T, Weiss J. Wetting and drying of concrete using aqueous solutions containing deicing salts. Cement Concr Compos 2011;33(5):535–42.
[4] Grosse CU, Finck F. Quantitative evaluation of fracture processes in concrete using signal-based acoustic emissions techniques. Cement Concr Compos 2006;28:330–6.
[5] Ohtsu M, Okamoto T, Yuyama S. Moment tensor analysis of AE for cracking mechanisms in concrete. ACI Struct J 1998;95(2):87–95.
[6] Carpinteri A, Lacidogna G, Manuello A. Damage mechanisms interpreted by acoustic emission signal analysis. Key Eng Mater 2007;347:577–82.
[7] Ohtsu M. Acoustic emission characteristics in concrete and diagnostic applications. J Acoust Emission 1987;6(2):99–108.
[8] Matsuyama K, Fujiwara T, Ishibashi A, Ohtsu M. Field application of acoustic emission for the diagnosis of structural deterioration of concrete. J Acoust Emission 1993;11:65–73.
[9] Shiotani T, Ohtsu M, Ikeda K. Detection and evaluation of AE waves due to rock deformation. Constr Build Mater 2001;15:235–46.
[10] Shah HR, Weiss J. Quantifying shrinkage cracking in fiber reinforced concrete using the ring test. Mater Struct 2006;39(9):887–99.

[11] Bolander JE, Hikosaka H, Shiraishi T. Effects of strain gradient on concrete tensile fracture, vol. 53, no. 3. Memoirs of the Kyushu University, Faculty of Engineering; 1993. p. 103–9
[12] Langenberg KJ, Mayer K, Marklein R. Nondestructive testing of concrete with electromagnetic and elastic waves: modeling and imaging. Cement Concr Compos 2006;28(4):370–83.
[13] Carpinteri A, Lacidogna G, Niccolini G. Critical behavior in concrete structures and damage localization by acoustic emission. Key Eng Mater 2006;312:305–10.
[14] Kurz J, Grosse CU. Strategies for reliable automatic onset time picking of acoustic emissions and of ultrasound signals in concrete. Ultrasonics 2005;43:538–46.
[15] Carpinteri A, Lacidogna G. Structural monitoring and integrity assessment of medieval towers. J Struct Eng (ASCE) 2006;132:1681–90.
[16] Tong C, Kennett BLN. Automatic seismic event recognition and later phase identification for broadband seismograms. Bull Seismol Soc Am 1996;86:1896–909.
[17] Baer M, Kradolfer U. An automatic phase picker for local and teleseismic events. Bull Seismol Soc Am 1897;77:1437–45.
[18] Akaike H. Information theory and an extension of the maximum likelihood principle. In: Petrov BN, Csaki F, editors. Second international symposium on information theory, Springer-Verlag; 1973. p. 267–81.
[19] Yokota T, Zhou S, Mizoue M, Nakamura I. An automatic measurement of arrival time of seismic waves and its application to an on-line processing system. Bull Earthquake Res Inst Tokyo Univ 1981;55:449–84.
[20] Zhang H, Thurber C, Rowe C. Automatic p-wave arrival detection and picking with multiscale wavelet analysis for single-component recordings. Bull Seismol Soc Am 2003;93 (5).
[21] Dai H, MacBeth C. The application of back-propagation neural network to automatic picking seismic arrivals from single-component recordings. J Geophys Res 1997;102(B7):15105–13.
[22] Boschetti F, Dentith MD, List RD. A fractal-based algorithm for detecting first arrivals on seismic traces. Geophysics 1996;61 (4).
[23] Xu J. P-wave onset detection based on the spectrograms of the AE signals. Adv Mater Res 2011;250–253:3807–10.
[24] Maeda N. A method for reading and checking phase times in auto-processing system of seismic wave data. Zisin 1985;38:365–79.
[25] Kitagawa G, Akaike H. A procedure for the modeling of non-stationary time series. Ann Inst Stat Math 1978;30 (351–363).
[26] Douglas A. Bandpass filtering to reduce noise on seismograms: is there a better way? Bull Seismol Soc Am 1997;87(3):770–7.
[27] Ohtsu M. Measurement method for acoustic emission signals in concrete. Mater Struct 2010;43:1177–81.